Hindawi
Journal of Chemistry
Volume 2020, Article ID 8820262, 9 pages
https://doi.org/10.1155/2020/8820262

Research Article

Preparation of Magnetic Molecularly Imprinted Polymers for Selective Recognition and Determination of Clenbuterol in Pork Samples

Yingjuan Zhao,[1] Zufei Feng,[1,2] Sijin Li,[1,2] Yan Lu,[1,2] Yangfan Hu,[1,2] Hua Fan,[1,2] and Xinyue Zhai[1]

[1]*Department of Applied Chemistry, Xi'an University of Technology, Xi'an 710048, China*
[2]*International Research Center for Composite and Intelligent Manufacturing Technology, Institute of Chemical Power Sources, School of Science, Xi'an University of Technology, Xi'an 710048, China*

Correspondence should be addressed to Zufei Feng; zufeifeng@xaut.edu.cn

Received 15 September 2020; Revised 29 October 2020; Accepted 31 October 2020; Published 17 November 2020

Academic Editor: Patricia E. Allegretti

Magnetic molecularly imprinted polymer (MMIP) was successfully synthesized with acrylamide as a functional monomer and clenbuterol (CLB) as a template molecule. The synthesized MMIPs were characterized by scanning electron microscopy (SEM), X-ray diffraction (XRD), and Fourier transform infrared spectrometry (FT-IR). MMIPs were used to identify and bind CLB as a solid phase extraction material. The experiment data were fitted by the Freundlich isotherm adsorption model. The results show that MMIPs have excellent recognition performance for CLB. MMIPs were successfully applied as adsorbents to preconcentrated CLB in pork samples and detected by HPLC with UV. The limit of detection (LOD) and limit of quantification (LOQ) were 4.27 μg/L and 14.2 μg/L, respectively. The spiked recovery rates ranged from 94.44% to 102.29%. Therefore, the prepared MMIPs can be used for selective preconcentration of CLB content in complex animal-derived food samples.

1. Introduction

Clenbuterol (CLB) is one of the most common β-adrenergic agonists that can be used in the treatment of diseases such as bronchial asthma and chronic bronchitis as a bronchodilator agent in the clinic treatment [1–3]. Moreover, a large amount of CLB can be used as feed additives to significantly promote the growth of the animal and increase the lean rate. It promotes the synthesis of proteins in muscles, especially skeletal muscles, and inhibits the synthesis of fat by changing the metabolic pathways in animals, thereby accelerating the growth rate, increasing the lean meat and improving the carcass quality. Therefore, CLB is also known as a lean meat agent [4–6].

As a feed additive, CLB can be used to increase the lean rate by using a large dose, which is usually more than 10 times that of human medicine. However, a large dosage, long use time, and slow metabolism will lead to a problem which is undesirable drug residues in animal-originated foodstuffs [7]. Long-term ingesting CLB from animal foods can cause abnormal physiological reactions such as dizziness, vomiting, muscle tremors, and even death [8]. In addition, illegal and uncontrolled use of CLB can also increase the environmental burden and cause environmental pollution [9]. The Chinese government clearly stipulates that the use of clenbuterol in pig breeding is prohibited. According to the Chinese government standard, clenbuterol should be no more than 0.01 mg kg^{-1}. Although many countries and regions have forbidden the use of CLB in livestock production, it has been still added in the fodder for animals to seek benefits [10–12]. Therefore, it is urgent to establish a simple, rapid, and efficient method to detect the residue of CLB to ensure food safety.

Currently, there have been several reports on methods for determining residue of CLB, such as biosensors, immunology, and chromatography [13]. However, all of the

above methods have more or fewer shortcomings. The limitation of biosensors [14] is the lack of stability and reproducibility. Immunological methods, such as flow immunoassay [15], immunochromatographic assay (ICA) [16], enzyme-linked immunosorbent assay (ELISA) [17], and time-resolved fluoroimmunoassay (TRFIA) [18], are less sensitive while the preparation, stability, and storage of antibodies always imply high costs [13]. Although the sample could be separated by chromatography and detected accurately by MS, time-consuming pretreatment, complex operation, and the high cost of the whole experiment are often cited as problems. Also, chromatography-mass spectrometry suffers from drawbacks of matrix effects which affect the selectivity, detection limits, maintenance frequency, and quantitative aspects. The most important shortcoming of these procedures is the lack of selectivity for target molecules. Moreover, the pretreatment of samples by these methods are mostly complicated.

In order to avoid the above weakness and promote advantages, researchers have been trying to establish new methods. Recently, molecular imprinting technology (MIT) has received more and more attention and is used in many fields, especially in solid phase extraction [19, 20]. It is a technique for adsorbing target molecules by preparing molecularly imprinted polymers (MIPs) with specificity and selectivity [21].

MIP is a three-dimensional network polymer with specific recognition and selective adsorption, which is usually synthesized by free-radical polymerization. First, the template molecule interacts with the functional monomer to form tailor-made binding sites; and then crosslinkers are distributed around the template molecules, which polymerize the highly crosslinked polymers. After the crosslinking reaction, the template molecules are eluted with a special solvent, the binding cavities which are capable of specifically recognizing the target molecules are revealed in the crosslinked material [22–26].

Alternatively, magnetic separation technology has also received a lot of attention due to its being fast, economical, and efficient [27–29]. When the magnetic separation technology and molecular imprinting technology are combined, the magnetic molecularly imprinted polymers (MMIPs) are formed. These MMIPs not only show excellent specific selective binding for target analytes but also can be quickly separated and easily recovered from the samples by an external magnet without centrifugation or filtration.

In this work, the MMIPs were synthesized and characterized as selective adsorbents for CLB. The Fe_3O_4 nanoparticles are encapsulated in the polymer to give it magnetic properties.

The kinetic studies and adsorption capacity on CLB adsorption by MMIPs were evaluated in detail. Finally, CLB was successfully preconcentrated by prepared MMIPs and detected with HPLC-UV in actual pork samples.

2. Materials and Methods

2.1. Materials and Reagents. Clenbuterol was purchased from Alfa Aesar (Tianjin, China). Ferric chloride ($FeCl_3{\cdot}6H_2O$) and ferrous chloride ($FeCl_2{\cdot}4H_2O$) were obtained from Fuchen Chemical Reagents Factory (Tianjin, China). Methacrylic acid (MAA), acrylamide (AM) styrene (St), ethylene glycol dimethacrylamide (EGDMA), and 2,2′-azobisissobutyronitrile (AIBN) were from Alfa Aesar (Tianjin, China). Polyethylene glycol (PEG-6000) and ammonium hydroxide were obtained from Tianjin Chemical Reagent Co. (Tianjin, China). Chromatographic grade methanol and acetonitrile were acquired from Merck Co. (Darmstadt, Germany). All other organic solvents and inorganic reagents were of analytical reagent grade and provided by local suppliers. Pock was purchased from the local supermarket (Xi'an, China). All HPLC solutions were filtered using a filter (HA-0.45 μm) before being injected into the HPLC system.

2.2. Instrumentation. The HPLC analyses system consisted of a Shimadzu LC-20A HPLC system, CBM-102 UV/Vis detector (Shimadzu, Japan) and a chromatographic workstation (Shimadzu, Japan). A Sino-Chrom ODS-AP column (4.6 mm × 150 mm, 5 μm) was applied. The mobile phase was 0.3% of triethylamine in aqueous solution (pH = 3 with phosphoric acid) and acetonitrile (85 : 15, v/v). The wavelength of detection, flow rate, and column oven temperature were 243 nm, 1.0 mL/min, and 30°C, respectively.

The micromorphology of MMIPs and MNIPs was detected by field emission scanning electron microscopy (SEM, JSM-6700F, TESCAN Co., Ltd., Czech). The infrared spectrum was measured by Fourier Transform Infrared spectrometer IR-960 (Rui'an Technology Co., Ltd., Tianjin, China). X-ray diffraction was carried out using XRD-6100 (Shimadzu, Japan). The shaken bed used the KYC 100B rocking incubator. The ultrasonic cleaner uses KQ-300B (Ultrasonic Instrument Co., Ltd., Kunshan, China).

2.3. Preparation of Fe_3O_4 Magnetic Particles. Fe_3O_4 magnetic particles were synthesized by improved chemical coprecipitation method according to the previous study [30, 31]. Briefly, $FeCl_3{\bullet}6H_2O$ (5.11 g) and $FeCl_2{\bullet}4H_2O$ (1.83 g) were dissolved in 80 mL of deoxygenated water in a 250 mL four-necked flask, and the mixture was constantly stirred under nitrogen protection.

Then 60 mL of ammonium hydroxide solution (5%) was added drop by drop when the temperature was raised to 80°C. The mixture was stirred vigorously for 60 min at 80°C. Subsequently, the Fe_3O_4 nanoparticles were collected by using an external magnet and washed with deionized water several times until the pH = 7.

The PEG-modified Fe_3O_4 was prepared according to previous work with some minor modifications. The prepared Fe_3O_4 (2.0 g) and PEG (10.0 g) were dissolved in deoxygenated water (30 mL) by stirring for 30 min and sonicating for 20 min to obtain the homogeneously dispersed solution, which was stored in a dark place for later use.

2.4. Preparation of the MMIPs. The MMIPs were prepared as follows: firstly, an appropriate amount of clenbuterol

(0.5 mmol), as the template molecule, and AM (4 mmol), as the functional monomer, were added to a glass flask containing 25 mL acetonitrile. Then, the mixture was stored in the dark for 18 h at room temperature to obtain the prepolymerization solution. After that, the prepolymerization solution and PEG-Fe_3O_4 particles were dispersed in 80 mL of doubly distilled water and copolymer monomer (St, 87.4 mmol), crosslinker (EDGMA, 30 mmol), and initiator (AIBN, 0.6 mmol) were added to the mixture in a 250 mL three-neck flask. The processed mixture was placed in a water bath and stirred for the polymerization at 70°C under nitrogen protection for 12 h. After polymerization, MMIPs were collected by an extra magnetic field and washed by a mixture of methanol-acetic acid (9 : 1, v/v) to remove the templates, and then rinsed with methanol. The synthesized MMIP (30 mg) was added to methanol (1 mL). After shaking for 15 min, HPLC was used to detect whether the template molecules were removed. Finally, the MMIPs were dried in a vacuum. For comparison, the nonimprinted polymers (NIPs) were also prepared as the same method mentioned above in the absence of the template.

2.5. Adsorption Capacity Experiment. To evaluate adsorption properties of MMIPs for clenbuterol, the batch adsorption test was performed as follows: 30 mg MMIPs or MNIPs were immersed into the 2 mL centrifuge tube containing methanol solution of clenbuterol (100–300 μg L^{-1}, 1 mL) followed by shaking for 15 min at room temperature. MMIPs or MNIPs were separated from the solution by using a magnet. The concentration of clenbuterol in the supernatant was analyzed by HPLC-UV after filtration through a 0.45 μm microporous membrane. In order to evaluate the binding parameters of MMIP and MNIP, the Freundlich isotherm (FI) model was further used to further process the data from the adsorption experiments.

In adsorption kinetics experiments, 30 mg of MMIPs and MNIPs were added to 1 mL of clenbuterol methanol solution (160 μg L^{-1}). The mixture was shaken mechanically for 5, 10, 15, 20, 30, 45, and 60 min in a shaken bed at room temperature to choose the optimal time of competitive adsorption.

2.6. Determination of CLB in Pork Samples. One hundred grams of pork (obtained from a local market) was broken with a tissue shredder in 100 mL pure water. Then MMIPs (30 mg) were added to the real sample homogenate solution (1 mL), followed by being shaken at 25°C for 15 min. And then, MMIPs were separated from the solution using an external magnet. The CLB was eluted from the MMIPs using 1 mL of methanol-acetic acid (9 : 1, v/v) solution. The eluted solution was filtered by a membrane filter (0.25 μm), dried by nitrogen flow, and dissolved in 0.1 mL of methanol for the detection by HPLC-UV analysis.

3. Results and Discussion

3.1. Preparation and Characterization of MMIPs. Figure 1 shows that the preparation process of MMIPs is mainly divided into two steps. The first is the synthesis of Fe_3O_4 nanoparticles. At present, the chemical coprecipitation method is widely used to prepare magnetic nanoparticles because of its simple operation and good reproducibility. Therefore, Fe_3O_4 nanoparticles are prepared by this method with superparamagnetism in this experiment. However, the prepared Fe_3O_4 nanoparticles are prone to magnetic flocculation, so that the result is that nanoparticles lack monodispersity. Therefore, the surface of Fe_3O_4 particles was modified with PEG to avoid electrostatic agglomeration.

In noncovalent molecular imprinting, the interaction between functional monomers and template molecules affects the recognition performance of MMIPs directly. Therefore, acrylamide (AM) and methacrylic acid (MAA) were selected as functional monomers to evaluate optimal one. In theory, both AM and MAA could produce hydrogen bonds with clenbuterol, but the experimental results show that the specific recognition ability of MMIPs synthesized with AM as a functional monomer is stronger. Further, styrene was used as a comonomer in this experiment because the unsaturated bond in its structure contributes to the formation of a crosslinked structure and increases the structural stability of the polymers.

SEM was used to measure the morphological features of MMIPs and MNIPs in Figure 2. As can be seen from the figure, the surface of the MMIPs is rough and porous, while the surface of the MNIPs is relatively regular. As a result, the porous surface and imprinting sites of the MMIPs are more conducive to specific adsorption than MNIPs.

X-ray diffraction patterns of MMIPs and Fe_3O_4 nanoparticles are shown in Figure 3. The curve shows five strong diffraction peaks at 20–80°, (220), (311), (400), (440), (511) crystal planes, which correspond with the Inorganic Crystal Structure Database (ICSD). The diffraction peaks of MMIPs are similar to Fe_3O_4 nanoparticles, proving that the polymers are compounds of Fe_3O_4 nanoparticles.

FT-IR was used to analyze the main functional groups of synthesized results. Figure 4 shows the infrared spectrum of Fe_3O_4 nanoparticles, MMIPs, and MNIPs. The typical bands at 3028 and 2933 cm^{-1} can be attributed to the C-H aromatic stretching vibrations of styrene units. The absorption peak of C = O at 1723.9 cm^{-1} is due to the crosslinking agent EGDMA reacted with AM. Compared with NIP, weak absorption peaks appeared at 1632.8 and 1599.8 cm^{-1}, which attributed to carbonyl and bending vibration of the imino group in $CONH_2$. It indicated that most AM and crosslinking agent had crosslinking polymerized during the preparation of MIPs, and only some AM residues were found. Compared to curve 3 (black), the band of Fe-O at 547.1 cm^{-1} was observed in MMIPs, which confirmed that Fe_3O_4 was implanted into the polymer network successfully.

3.2. Adsorption and Analytical Kinetic Evaluation. An adsorption kinetics experiment was performed on MMIPs to select the best extraction time. Figure 5(a) shows that the amount of adsorption increased sharply in the first 15 min. The adsorption equilibrium was reached at 15 min, and the maximum adsorption amount was obtained, so 15 min was selected as the extraction time.

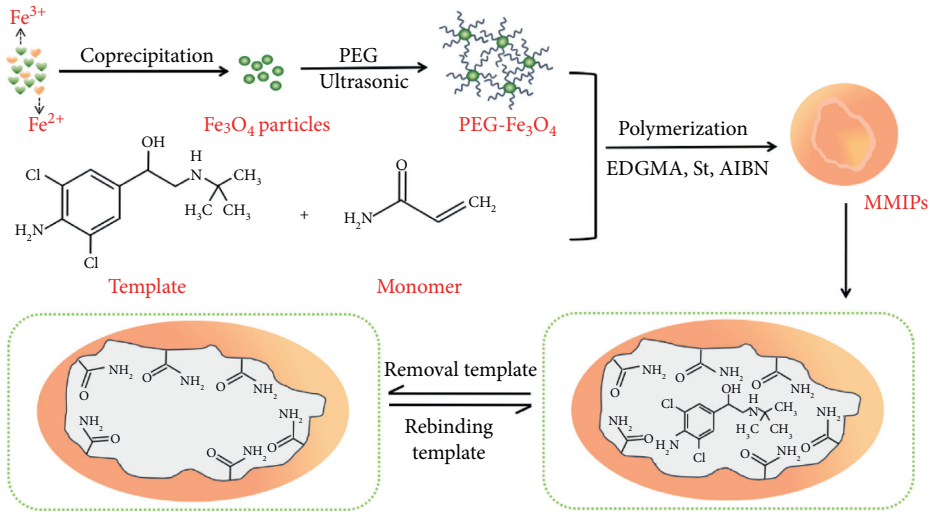

Figure 1: Schematic preparation procedure for CLB MMIPs.

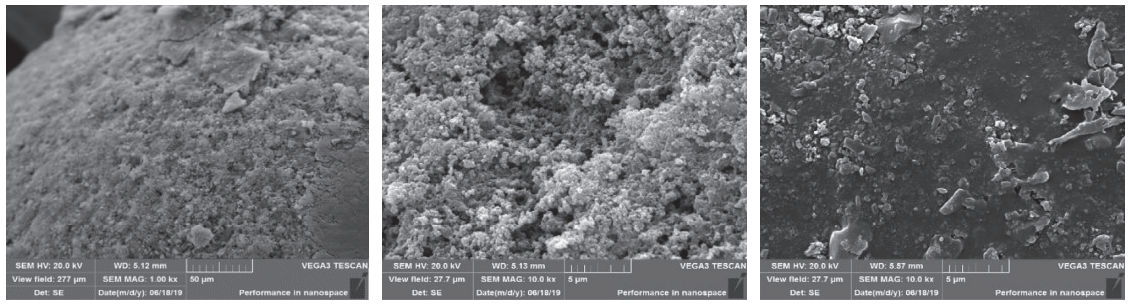

Figure 2: Scanning electron micrographs of the MMIPs and MNIPs: (a) MMIPs; (b) surface of MMIPs; (c) surface of MNIPs.

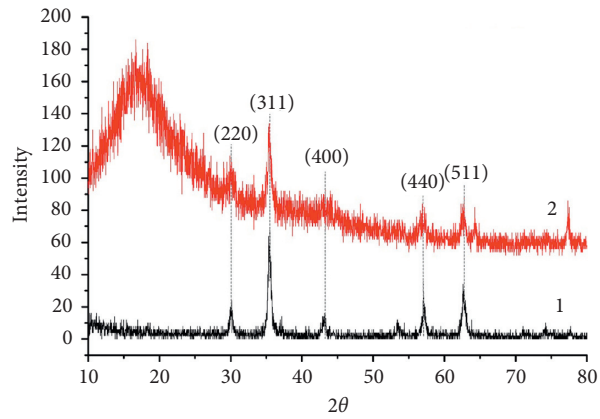

1: Fe_3O_4
2: MMIP

Figure 3: XRD patterns of the Fe_3O_4 (1) and MMIPs (2).

Figure 5(b) shows the desorption kinetics of CLB by MMIP, and the desorption time was optimized. After 15 min, the desorption ratio is close to 100%. After desorption, MMIPs can be quickly separated and recovered from the sample solution by an external magnetic field.

3.3. Adsorption Isotherm Equation. To assess the binding energy, binding site type and distribution between MMIPs or MNIPs and imprinted molecules, adsorption isotherms were adopted using different concentrations of CLB. Figure 6(a) shows the adsorption isotherms of MMIPs and

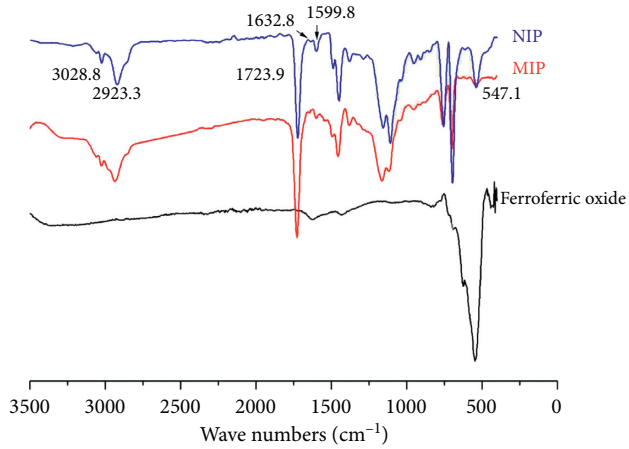

Figure 4: FT-IR spectra of MMIP (red), MNIP (blue), and Fe_3O_4 magnetic nanoparticles (black).

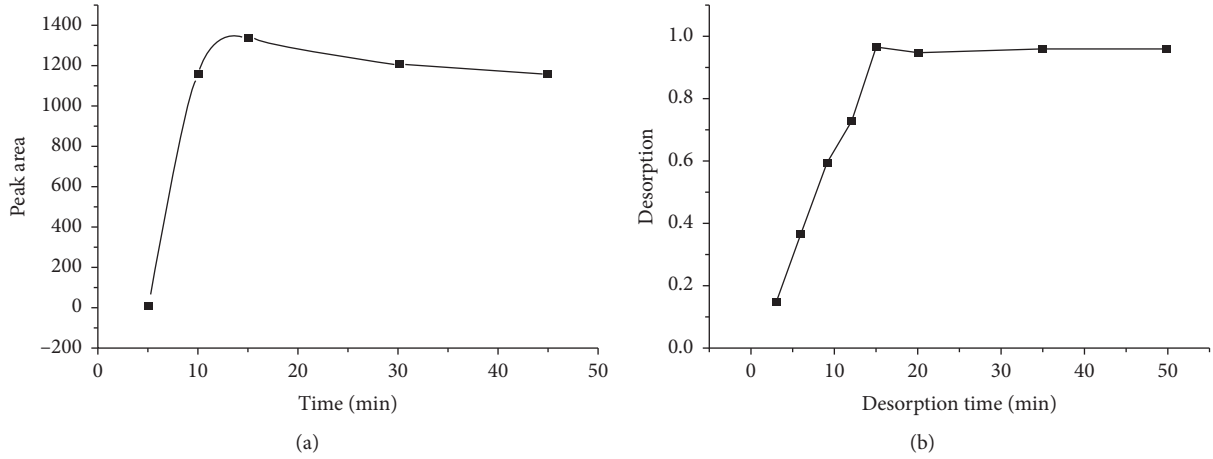

Figure 5: (a) Effect of adsorption time; (b) effect of desorption time.

MNIPs. When the adsorption reaches equilibrium, there is a certain relationship between the adsorption amount B and the residual amount F. It is possible to observe an increase of adsorption amount of polymer materials with increasing of the initial concentration of CLB, and the adsorption capacity of MMIPs for CLB is greater than that of MNIPs. Some studies have shown that the Freundlich equation has good applicability to noncovalently imprinted materials [30, 32]. Therefore, the Freundlich isothermal (FI) adsorption model was adopted to analyze the data with adsorption isotherms.

The FI equation is expressed as follows [32]:

$$B(F) = aF^m, \tag{1}$$

where B and F are the concentrations of bound and free analyte, respectively; a and m are characteristic parameters of the Freundlich isotherm equation: a is the total number of binding sites, which represents the adsorption capacity of the adsorbent; m is the heterogeneity index with a value from 0–1. The value of m closes to 0 or 1 indicates that the adsorption sites are heterogeneous and homogeneous, respectively. And the value of a and m can be obtained from the following equation:

$$\log B = m \log F + \log a. \tag{2}$$

The number of binding sites with given affinity ($N(k)$) of a polymer can be calculated by equation (3), where K is the affinity constant, $K = 1/F$.

$$N(K) = 2.303am\left(1 - m^2\right)K^{-m}. \tag{3}$$

The binding site $N_{k\,\min-k\,\max}$ and the apparent average binding constant $K_{k\,\min-k\,\max}$ per gram of polymer can be calculated from equation (4) and equation (5), respectively.

$N_{k\,\min-k\,\max}$ is the number of binding sites per gram of polymer. $K_{k\,\min-k\,\max}$ is apparent average binding constant. They can be calculated from equation (4) and equation (5), respectively, where $K_{\min} = 1/F_{\max}$; $K_{\max} = 1/F_{\min}$. $F_{\max}$ and $F_{\min}$ are the maximum and minimum solute concentrations of the liquid phase at adsorption equilibrium, respectively; a and m are the characteristic parameters of the Freundlich isothermal equation.

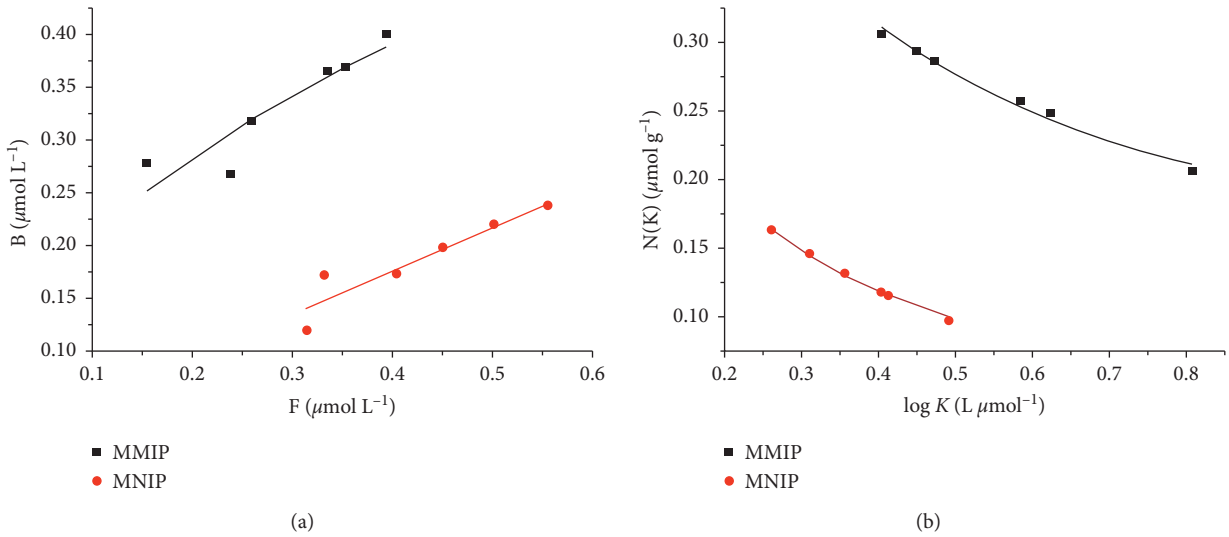

Figure 6: (a) CLB adsorption isotherms for MMIPs and MNIPs with the corresponding experimental FI for MMIPs and MNIPs; (b) affinity distributions of MMIPs (black curve) and MNIPs (red curve).

Table 1: Characteristic parameters of the Freundlich isothermal equation.

Fitting parameters	MMIPs	MNIPs
a	0.568	0.432
m	0.426	0.985
K_{range} (L μmol^{-1})	2.541–6.442	1.799–3.184
$N(K)$ (μmol g^{-1})	0.206–0.307	0.009–0.017
$N_{k\,min-k\,max}$ (μmol g^{-1})	0.220	0.003
$K_{k\,min-k\,max}$ (L μmol^{-1})	4.067	2.358

$$N_{k\,min-k\,max} = a\left(1 - m^2\right)\left(K_{min}^{-m} - K_{max}^{-m}\right), \quad (4)$$

$$K_{k\,min-k\,max} = \left(\frac{m}{m-1}\right)\left(\frac{K_{min}^{1-m} - K_{max}^{1-m}}{K_{min}^{-m} - K_{max}^{-m}}\right). \quad (5)$$

The FI affinity distribution model was further used to analyze the adsorption data. The affinity distribution curve (Figure 6(b)) was obtained by plotting the value of $N(k)$ and $\log K$, indicating the number of binding sites with binding ability. The value of $\log K$ represents the binding energy as the abscissa. It can be seen from the figure that the number of binding sites of MMIPs is always higher than that of MNIPs when given the binding energy within the experimental concentration range. It indicates that there are specific adsorption sites in the MMIPs material, and the imprinting effect is evident.

The results are exhibited in Table 1. The total number of binding sites and binding constants of MMIPs is higher than MNIPs. The binding sites N, K of MMIPs per gram of polymer are larger than MNIPs. These results indicate that the target molecule plays an important role in the formation of specific sites during the imprinting process.

3.4. Method Validation. In order to verify the accuracy of the method, the linear relationship, correlation coefficient (r), the limit of detection (LOD), the limit of quantification (LOQ), and spiked recovery experiment were investigated. By drawing the standard curve, the linear regression equation is $y = 7.724x + 278$ ($r = 0.9694$) (Figure 7). The values of LOD and LOQ were measured to be 3 and 10 times the signal-to-noise ratio (S/N), respectively. Their values were 4.27 and 14.2 μg L^{-1}.

At the same time, the spiked sample recovery experiment was used to assess the reproducibility and accuracy of the method. Three different concentrations of samples were added to the CLB samples, and the recovery was measured and calculated. The concentration of the base solution is 0.25 μmol L^{-1}. The recovery values were calculated by the formula below:

$$\text{Recovery} = \left[\frac{(\text{Found} - \text{base})}{\text{added}}\right] \times 100\%. \quad (6)$$

The results were shown in Table 2. The recoveries ranged from 94.44 to 102.29%, and the relative standard deviation (RSD) ranged from 3.48 to 7.14%. The same sample was measured 5 times and the RSD was calculated to be 4.93%.

$$a\left[\frac{(\text{Found} - \text{base})}{\text{added}}\right]100\%. \quad (7)$$

3.5. Analysis of Real Samples. In order to investigate the extraction and enrichment ability of MMIPs on actual

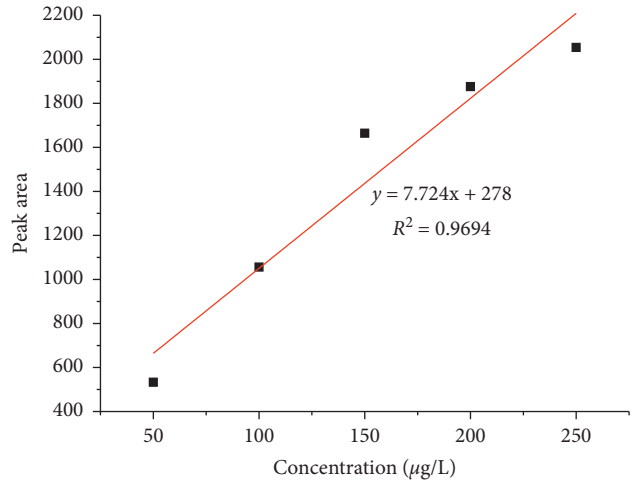

Figure 7: The standard curve with linear regression.

Table 2: Accuracy of the method for sample solutions spiked at different concentrates ($n = 3$).

Samples	Added (μmol L^{-1})	Found (μmol L^{-1})	Recovery (%[a])	Average (%)	RSD (%)
CLB	0.18	0.45	111.11	94.44	7.14
	0.18	0.39	77.77		
	0.18	0.42	94.44		
	0.29	0.55	103.44	97.70	5.38
	0.29	0.52	93.10		
	0.29	0.53	96.55		
	0.36	0.58	91.66	96.29	3.48
	0.36	0.62	102.77		
	0.36	0.59	94.44		

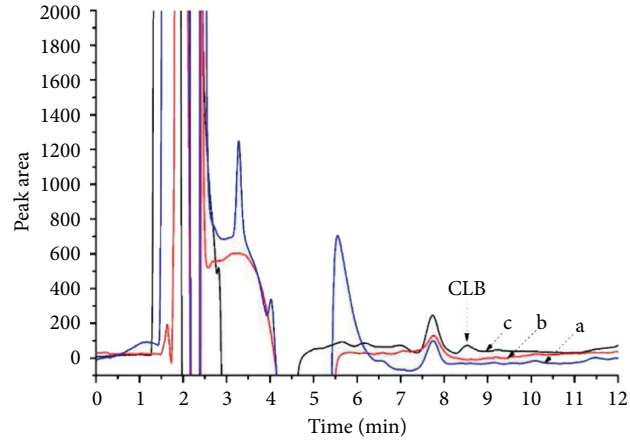

Figure 8: HPLC-UV chromatograms of pork samples without enrichment (a), enrichment by MNIPs (b) and MMIPs (c).

samples, we extracted and detected CLB in pork according to the method of section 2.5 and realized the analysis and detection of trace components from the matrix.

The chromatogram of the pork sample extracted by MMIPs (Line a) and MNIPs (Line b) and direct injection of the sample without enrichment (Line c) are shown in Figure 8. Figure 8(a) shows that CLB cannot be detected directly because the concentration is low without enrichment. Figure 8(b) also shows the sample could not be extracted by MNIPs, which proves that its enrichment is nonspecific adsorption. Figure 8(c) shows that a higher peak appeared and highly selective adsorption was achieved after the sample was extracted by MMIPs. The content of CLB in pork was calculated resulting in $9.87 \pm 0.48\,\mu g\ kg^{-1}$. The result showed that MMIPs could be used to enrich and detect CLB in actual samples.

4. Conclusions

In summary, this study synthesized MMIPs of CLB for the first time. The synthesized MMIPs were characterized by SEM, FT-IR, and XRD. Adequate Fe_3O_4 nanoparticles are coated in the MMIPs, which ensures that the MMIPs can be easily and quickly separated from the complex solution through an external magnetic field without centrifugation or filtration. Through isothermal adsorption experiments, it was confirmed that MMIPs have good specific recognition and selective adsorption ability. The high recovery of spiked recovery experiments demonstrates that this approach is effective. Therefore, the method can be used for the residue detection of clenbuterol in animal products such as pork or pig urine.

Data Availability

The authors confirm that all data underlying the findings of this study are fully available without restriction.

Conflicts of Interest

The authors declare no conflicts of interest.

Acknowledgments

This work was financially supported by the National Natural Science Foundation of China (no. 81302619); Key Programs (nos. 2018JM7104 and 2018JQ2050), and Innovation Capability Support Program (no. 2019TD-019) funded by Science and Technology Department of Shaanxi Provincial Government; Natural and Scientific Program (nos. 20JK0804, 19JK0572, and 17JK0554) funded by Education Department of Shaanxi Provincial Government.

References

[1] G. J. Garssen, G. H. Geesink, A. H. Hoving-Bolink, and J. C. Verplanke, "Effects of dietary clenbuterol and salbutamol on meat quality in veal calves"" *Meat Science*, vol. 40, no. 3, pp. 337–350, 1995.

[2] N. González, M. Grünhut, I. Šrámková et al., "Flow-batch analysis of clenbuterol based on analyte extraction on molecularly imprinted polymers coupled to an in-system chromogenic reaction. Application to human urine and milk substitute samples," *Talanta*, vol. 178, pp. 934–942, 2018.

[3] G. Brambilla, T. Cenci, F. Franconi et al., "Clinical and pharmacological profile in a clenbuterol epidemic poisoning of contaminated beef meat in Italy," *Toxicology Letters*, vol. 114, no. 1–3, pp. 47–53, 2000.

[4] B. Zhang, X. Fan, and D. Zhao, "Computer-aided design of molecularly imprinted polymers for simultaneous detection of clenbuterol and its metabolites," *Polymers*, vol. 11, no. 1, p. 17, 2018.

[5] Z. Huang, Z. Xiong, Y. Chen, S. Hu, and W. Lai, "Sensitive and matrix-tolerant lateral flow immunoassay based on fluorescent magnetic nanobeads for the detection of clenbuterol in swine urine," *Journal of Agricultural and Food Chemistry*, vol. 67, no. 10, pp. 3028–3036, 2019.

[6] H. J. Mersmann, "Overview of the effects of beta-adrenergic receptor agonists on animal growth including mechanisms of action," *Journal of Animal Science*, vol. 76, no. 1, pp. 160–172, 1998.

[7] L. Zhang, Q. Wang, Y. Qi, L. Li, S. Wang, and X. Wang, "An ultrasensitive sensor based on polyoxometalate and zirconium dioxide nanocomposites hybrids material for simultaneous detection of toxic clenbuterol and ractopamine," *Sensors and Actuators B: Chemical*, vol. 288, pp. 347–355, 2019.

[8] T. Y. K. Chan, "Health hazards due to clenbuterol residues in food," *Journal of Toxicology: Clinical Toxicology*, vol. 37, no. 4, pp. 517–519, 1999.

[9] F. C. Cabello and H. P. Godfrey, "Even therapeutic antimicrobial use in animal husbandry may generate environmental hazards to human health," *Environmental Microbiology*, vol. 18, no. 2, pp. 311–313, 2016.

[10] P. E. Strydom, L. Frylinck, J. L. Montgomery, and M. F. Smith, "The comparison of three β-agonists for growth performance, carcass characteristics and meat quality of feedlot cattle," *Meat Science*, vol. 81, no. 3, pp. 557–564, 2009.

[11] X. Zhang, H. Zhao, Y. Xue et al., "Colorimetric sensing of clenbuterol using gold nanoparticles in the presence of melamine," *Biosensors and Bioelectronics*, vol. 34, no. 1, pp. 112–117, 2012.

[12] A. M. M. Niño, H. M. M. Granja Rodrigo, C. Wanschel Amarylis, and G. Salerno Alessandro, "The challenges of ractopamine use in meat production for export to European Union and Russia," *Food Control*, vol. 72, pp. 289–292, 2015.

[13] M. X. Xu, W. Li Zhao, J. Liu, T. He, J. J. Huang, and J. P. Wang, "Determination of β-agonists in porcine urine by molecularly imprinted polymer based chemiluminescence," *Analytical Letters*, vol. 52, no. 11, pp. 1771–1787, 2019.

[14] B. Bo, X. Zhu, P. Miao et al., "An electrochemical biosensor for clenbuterol detection and pharmacokinetics investigation," *Talanta*, vol. 113, no. 17, pp. 36–40, 2013.

[15] Y. Cong, H. Dong, X. Y. Wei et al., "A novel murine antibody and an open sandwich immunoassay for the detection of clenbuterol," *Ecotoxicology and Environmental Safety*, vol. 182, Article ID 109473, 2019.

[16] Q. Yu, J. Liu, G. Zhao, and W. Dou, "A silica nanoparticle based 2-color immunochromatographic assay for simultaneous determination of clenbuterol and ractopamine," *Microchimica Acta*, vol. 186, no. 7, p. 421, 2019.

[17] Q. Huang, B. Zhao, S.-E. Bold et al., "Immunoassay of clenbuterol with bacteria as natural signal carriers for signal amplification," *Sensors and Actuators B: Chemical*, vol. 288, pp. 210–216, 2019.

[18] S. Fang, Y. Zhang, X. Liu, J. Qiu, Z. Liu, and F. Kong, "Development of a highly sensitive time-resolved fluoroimmunoassay for the determination of trace salbutamol in environmental samples," *Science of The Total Environment*, vol. 679, pp. 359–364, 2019.

[19] G. Brambilla, M. Fiori, B. Rizzo, V. Crescenzi, and G. Masci, "Use of molecularly imprinted polymers in the solid-phase extraction of clenbuterol from animal feeds and biological matrices," *Journal of Chromatography B: Biomedical Sciences and Applications*, vol. 759, no. 1, pp. 27–32, 2001.

[20] N. Kumar, N. Narayanan, and S. Gupta, "Application of magnetic molecularly imprinted polymers for extraction of imidacloprid from eggplant and honey," *Food Chemistry*, vol. 255, pp. 81–88, 2018.

[21] Z. Li, Z. Cui, Y. Tang et al., "Fluorometric determination of ciprofloxacin using molecularly imprinted polymer and polystyrene microparticles doped with europium(III)(DBM) 3phen," *Mikrochimica Acta*, vol. 186, no. 6, p. 334, 2019.

[22] S. Ansari, "Application of magnetic molecularly imprinted polymer as a versatile and highly selective tool in food and environmental analysis: recent developments and trends," *TrAC Trends in Analytical Chemistry*, vol. 90, pp. 89–106, 2017.

[23] P. Wang, J. Liu, X. Chen et al., "Janus silica nanosheets-based MMIPs platform for synergetic selective capture and fast separation of 2′-deoxyadenosine: two different components segmented on the surface of one object," *Chemical Engineering Journal*, vol. 369, pp. 793–802, 2019.

[24] L. N. M. Saavedra, B. E. L. Baeta, M. C. Pereira, L. C. A. de Oliveira, and A. C. da Silva, "Thermodinamic study of a magnetic molecular imprinted polymer for removal of nitrogenous pollutant from gasoline," *Fuel*, vol. 210, pp. 380–389, 2017.

[25] X. Li, Y. Dai, and K. H. Row, "Preparation of two-dimensional magnetic molecularly imprinted polymers based on boron nitride and a deep eutectic solvent for the selective recognition of flavonoids," *The Analyst*, vol. 144, no. 5, pp. 1777–1788, 2019.

[26] L. Ye, "Synthetic strategies in molecular imprinting," *Molecularly Imprinted Polymers in Biotechnology*, vol. 150, pp. 1–24, 2015.

[27] Y. Poo-arporn, S. Pakapongpan, N. Chanlek, and R. P. Poo-arporn, "The development of disposable electrochemical sensor based on Fe_3O_4-doped reduced graphene oxide modified magnetic screen-printed electrode for ractopamine determination in pork sample," *Sensors and Actuators B: Chemical*, vol. 284, pp. 164–171, 2019.

[28] Y. Sun, T. Fu, S. Chen et al., "A novel colorimetric immunosensor based on platinum colloid nanoparticles immobilized on PowerVision as signal probes and Fe_3O_4 @ β-cyclodextrin as capture probes for ractopamine detection in pork," *Journal of the Science of Food and Agriculture*, vol. 99, no. 6, pp. 2818–2825, 2019.

[29] S. Chen, J. Fu, Z. Li et al., "Preparation and application of magnetic molecular imprinted polymers for extraction of cephalexin from pork and milk samples," *Journal of Chromatography A*, vol. 1602, pp. 124–134, 2019.

[30] Z. Feng, Y. Lu, Y. Zhao, and H. Ye, "Fast extraction and detection of 4-methylimidazole in soy sauce using magnetic molecularly imprinted polymer by HPLC," *Molecules*, vol. 22, no. 11, p. 1885, 2017.

[31] Z. Feng, Y. Xu, S. Wei, B. Zhang, F. Guan, and S. Li, "Fabrication of Fe_3O_4 nanoparticle-coalesced hydroxylated multi-walled carbon nanotubes for the analysis of strychnine in human serum," *Analytical Sciences*, vol. 31, no. 5, pp. 399–406, 2015.

[32] A. M. Rampey, R. J. Umpleby, G. T. Rushton, J. C. Iseman, R. N. Shah, and K. D. Shimizu, "Characterization of the imprint effect and the influence of imprinting conditions on affinity, capacity, and heterogeneity in molecularly imprinted polymers using the freundlich isotherm-affinity distribution analysis," *Analytical Chemistry*, vol. 76, no. 4, pp. 1123–1133, 2004.